Auralization model for the perceptual evaluation of tyre–road noise

Auralization model for the perceptual evaluation of tyre–road noise

Jens Forssén, Alice Hoffmann, Wolfgang Kropp

Division of Applied Acoustics, Chalmers University of Technology, SE-41296 Gothenburg, Sweden

Abstract

Due to improvements in combustion-engines and use of electric-engines for cars, tyre noise has become the prominent noise source also at lower speeds. Models exist that simulate the noise produced by a rolling tyre, as do models that auralize different traffic situations from basic data. In this paper, a novel auralization method is introduced, with the purpose to enable synthesis of useful car pass-by sound signals for various situations. The method is based on an established model for tyre noise levels (SPERoN) that is combined with a validated auralization tool (LISTEN). In the LISTEN approach, source signals for tyre–road interaction and propulsion are produced from data based on recorded pass-by sounds. In the combined model, the tyre–road interaction data is shaped by the spectra estimated in SPERoN and synthesized back into a pass-by signal. The combined model is made to agree spectrally with measurements for a receiver at 7.5 m distance. Psychoacoustic judgments were used to compare the modelled signals with recorded signals, and the pass-by sounds for a given listener position showed promising quality and accuracy with respect to perceived pleasantness.

1. Introduction

Tyre–road noise is the main source of road traffic noise for driving speeds above 30 km/h [1]. This means that the expected transition to electric vehicles will not make a difference when it comes to the yearly more than one million lost healthy years in Western Europe [2]. Despite the importance of tyre–road noise, its reduction is progressing slowly due to at least two reasons. Firstly, the task to reduce tyre–road noise is very complex and there exists no simple solution. The design process of tyres has to include a multitude of performance criteria such as rolling resistance, handling and wet grip. It is not obvious that there are solutions that meet all demands and offer lower noise levels than today's tyres. In addition, tread pattern optimisation has been utilised for many years. Consequently, it might already today be close to optimal. Second, although the biggest potential for noise reduction is offered by low-noise road surfaces, they are costly and the lifetime of such surfaces is still losing to the lifetime of conventional surface types not optimised for tyre–road noise reduction.

To conclude, tyre–road noise will also in the future be an economical burden for society. Therefore, it is essential that the reduction of tyre–road noise is carried out as efficiently as possible. One factor in this context is the definition of the goal function for tyre–road noise reduction. Today, controlled pass by measurements (CPB) or close proximity measurements (CPX) are used to characterise tyre–road noise in-situ. In addition, tyre manufacturers use drum measurements for the characterisation of individual tyres. In all cases A-weighted levels are used. Both in measurements and simulations, A-weighted levels can easily be obtained. However, it is reasonable to assume that the A-weighted level is not a good descriptor for the perception of tyre–road noise. It can give an estimate of the perceived sound intensity, but to describe the perception of a sound, far more aspects need to be considered in general, such as those relating to perceived loudness, roughness, sharpness, fluctuation strength, and pitch. For evaluating the perception, audible signals are needed, which are then to be assessed in listening tests with respect to these psychoacoustic parameters. Existing situations can

easily be evaluated based on e.g. binaural recordings. For the design of new and innovative solutions, however, the signals have to be simulated (auralized) including all relevant aspects required to create realistic audible signals, e.g. for a pass-by situation.

The purpose of this paper is to describe a tool for auralizing tyre–road noise in a pass-by situation, based on proper descriptions of sources and propagation paths from a moving vehicle to a listener, as well as to demonstrate its functioning in a listening test comparing auralized sounds with recorded sounds. The auralization tool uses a combination of two models. The first model concerns the auralization of pass-by sound form road vehicles, developed in the LISTEN project (referred to as the LISTEN model in the following) [3-5]. Section 2 describes the methodology of the LISTEN model. The second model concerns the prediction of tyre–road noise levels for different combinations of tyres and road surfaces. This model is built on work made inside the so-called Sperenberg project [6] and is known as the SPERoN model. Section 3 describes the approach behind the SPERoN model. A comprehensive description of the two models is included here, which is not part of previous reviewed literature.

The combined model, described in Section 4, allows for simulating and auralizing pass-by sounds for arbitrary tyre and road combinations, as long as dense road surfaces are considered. A very first listening test is presented in Section 5 to demonstrate the functioning of the approach.

2. Approach for auralization

The approach for auralizing road vehicles as presented here uses previously published works as starting point, mainly by Maillard & Martin [7] and Kaczmarek [8]. Since then, more advanced approaches have been developed, e.g. works by Jagla et al. [9] and Pieren et al. [10]. Compared with the latter works, which can model accelerating vehicles, the LISTEN approach has a less advanced propulsion modelling which only allows for constant speeds in its current state. On the other hand, the LISTEN approach has been successfully validated (see Section 2.4) and the combined model as presented here has a wider capability of modelling tyre–road sounds than previous models. It could be noted also that, whereas most work has been focussing on light vehicles, heavy vehicles have started to be considered [11]. The combined model presented here can be further developed to consider also accelerating vehicles.

2.1 General approach

For the environmental sounds of interest here, linear acoustics theory can be assumed, whereby the source signal and the propagation effects can be separated. For a time signal, $s(t)$, of an omnidirectional point source, the sound pressure at the point of the receiver (i.e. the listener), $p(t)$, can be calculated as

$$p(t) = \int_0^\infty s(t-\tau)\,h(\tau)\,\mathrm{d}\tau \qquad \text{Eq 1}$$

where $h(\tau)$ is the impulse response due to the propagation.

As an example, the impulse response of free-field propagation in three-dimensional space can be written as the free-field Green function $h(\tau) = \delta(\tau - R/c)/4\pi R$, where $\delta(\tau)$ is the Dirac delta function, R is the distance, and c is the speed of sound. This results in a received sound signal according to

$$p(t) = \frac{s(t - R/c)}{4\pi R} \,. \qquad \text{Eq 2}$$

The resulting pressure signal according to Eq. (2) describes a delay in time of the source signal by an amount equal to R/c and a decrease in amplitude inversely proportional to distance, R. For a moving source the distance becomes a function of time, $R(t)$. The retarded time, $t - R(t)/c$, is used in the LISTEN approach to model the Doppler shift, via a resampling of the time signal.

In the processes of auralizing surface transport (road or rail), for a person standing still at a position exterior to the vehicle, a number of parameters need to be considered. The sound path (or paths) that reaches the listener from a vehicle can be described as starting from a set of sources that each has its own properties concerning source signal and directivity. While propagating from source to receiver, the sound will be influenced by changed amplitude due to: spherical spreading, air attenuation (leading to a larger reduction at the higher frequencies compared to at the lower frequencies) and the reflection on the ground surface (leading to an interference pattern over frequency). For the moving source, relative to the receiver, the Doppler effect needs to be modelled as described above. Such modelling may also be applied to consider a moving receiver, which is not implemented in this work, however.

Finally, the sound entering our ears is influenced by our head and torso, which here is modelled using head related transfer functions, HRTFs. The whole auralization process can, in our methodology, be summarized as starting with the synthesis of the source signals followed by the modelling of the air attenuation, the ground effect, the directivity, the Doppler effect, the spherical spreading and ending with the HRTFs. Modelling in third-octave bands is undertaken for the air attenuation, the ground effect and the directivity, whereas the Doppler effect and the spherical spreading is applied directly to the time signal. It could be noted that the spectral shift induced by Doppler shifting is assumed to lead to negligible alteration of the air attenuation and ground effect since they are relatively smooth functions of frequency, whereby the Doppler effect is here applied afterwards for simplicity. When different Doppler shifts are to be modelled for the direct and the ground reflected waves, as often wanted for aircraft auralization, a different approach could be applied (e.g. [12]). For the third-octave band filtering, an implementation in Matlab has been made that filters the input signal into the 30 bands from 25 Hz to 20 kHz (using a filter bank of 128th order FIR bandpass filters). The sampling rate used here is 44.1 kHz and the third-octave band propagation conditions are updated every thousand sample and then interpolated to the full sampling rate.

2.2 Modelling the ground effect and air attenuation

The results from the Nord2000 project [13] and the EU project Harmonoise [14] give a useful and solid physical basis for sound propagation modelling. Therefrom, the modelling of the effect of a flat ground is taken and entered here in the frequency domain, as well as the air attenuation, which is calculated according to the ISO-9613 standard [15]. Also, effects of refraction can be modelled to some degree of accuracy (i.e. curving of ray paths due to wind or varying temperature with height), whereas this is so far not considered here, due to the shorter ranges of propagation of current interest. For these cases, the models of the two projects Harmonoise and Nord2000 are very similar. Furthermore, for the combined case of two ground types, e.g. the asphalt of the

road and a grass lawn, the engineering approach of Fresnel weighting can be used, where the Fresnel weights depend on the sound frequency and the point of reflection of sound rays in relation to the position of the ground impedance jump [16].

Whereas Eq. 2 describes, in the time domain, the delay and the amplitude decay due to spherical spreading, the effects modelled in the frequency domain can be written as a gain in dB relative to free field,

$$\Delta L = \Delta L_{airatt} + \Delta L_{ground} + \Delta L_{extra} \quad \text{Eq 3}$$

where the total effect may be composed of the air attenuation, ΔL_{airatt}, the ground effect, ΔL_{ground}, and possibly other effects, ΔL_{extra}, e.g. due to screening, refraction and reflections on buildings. These gains are a function of the centre frequencies of the used third-octave bands. The ground effect can be written as

$$\Delta L_{ground} = 10\log_{10}\left\{1 + |Q|^2\frac{R_1^2}{R_2^2} + 2|Q|\frac{R_1}{R_2}\cos[k(R_2 - R_1) + \varphi]\cdot C\right\} \quad \text{Eq 4}$$

where $Q = |Q|e^{-j\varphi}$ is the spherical reflection factor with phase delay φ (using the $e^{j\omega t}$ convention), R_1 the direct distance, R_2 the reflected distance, k the wave number, $k = 2\pi f/c$, with f the sound frequency and c the sound speed, and where C is the coherence factor.

The coherence factor models the level of decorrelation between the direct and the ground reflected contributions, fulfilling $0 \leq C \leq 1$, where $C = 0$ means uncorrelated contributions and $C = 1$ means fully correlated contributions (e.g. [17]). This is further described in a paper detailing the Harmonoise model [16], where a different, but equivalent, notation is used, according to

$$\Delta L_{ground} = 10\log_{10}\{|1 + CQD|^2 + (1 - C^2)|QD|^2\} \quad \text{Eq 5}$$

with $D = \exp[-jk(R_2 - R_1)]\cdot R_1/R_2$. It is of importance to include the reduced coherence, which is naturally caused by random ground roughness and air turbulence, to avoid the extreme dips that the interference pattern for a point source and a point receiver may exhibit. This is especially valuable for the inversion process applied to find the source signal from a pass-by recording (as described in the following Subsection) since else the predicted dips would lead to erroneous peaks of the source spectrum. Here, a coherence loss due to turbulence is applied (assuming a Gaussian model for temperature fluctuations with a correlation length of 1 m and a normalized temperature variance of $8\cdot10^{-5}$, see e.g. [18]), as well as a correction that models the use of discrete frequencies [14]. Further description is found in [16]. It could be noted that when different Doppler shifts are to be modelled for the direct and the ground reflected waves a partly different approach could be applied [12].

For the air attenuation, we have used input values according to: 40 % relative humidity, temperature 24°C, and a static atmospheric pressure of 101.325 hPa. The ground has been modelled as dense asphalt, using a value of the effective flow resistivity of $2\cdot10^8$ Nsm^{-4} [13]. The used sound speed is $c =$ 340 m/s.

2.3 Modelling of the acoustic sources of road vehicles

To define the acoustic sources with their signals and direction-varying strengths (i.e. directivity), an inversion process is applied where a single recorded sound pressure signal is used as input. Similar approaches have been published previously [8,7]. Here,

we used five pass-by speeds, ranging from 30 to 110 km/h [3]. The process going from the mono recording to the source signal can be described as inverting or undoing the effects of the Doppler shift, the spherical spreading, the air-attenuation and the ground effect. A constant speed motion along a straight path is assumed for a single source location at centre of driving lane. With time for closest point of passage, distance to receiver, and vehicle speed as input, the propagation effects can be estimated at any time of the recorded pass-by sample. The signal is resampled to invert the Doppler effect and multiplied by the distance to invert the effect of spherical spreading on amplitude. The air attenuation is calculated at the third-octave band centre frequencies and applied to the respective third-octave band filtered channels of the recording. The recordings need to be made in a setting with low enough background noise level such that the signal to noise ratio is sufficient within the pass-by duration of interest.

Concerning the ground effect, for each road vehicle, two source heights are used in the modelling: (*i*) a propulsion source, which models engine, air intake, air exhaust, fans, compressors, etc.; and (*ii*) a tyre–road source, which models the noise generated by the contact between tyre and road surface. This is according to the engineering methods Harmonoise and Nord2000 [14,19], with the sources for passenger cars located at heights (*i*) 0.3 m and (*ii*) 0.01 m. (For medium heavy and heavy vehicles the height of the propulsion source is 0.75 m.) A transition frequency, where the tyre–road source is assumed to start dominating, is estimated from the Harmonoise source model [14]. The third-octave band of the used filter bank, which contains the transition frequency, together with bands above, are designated as tyre–road source whereas the lower bands are designated as propulsion source. The consequences of this approximation to be noted are that possible low-frequency aerodynamic noise is designated as propulsion noise and that possible high-frequency propulsion noise is designated as tyre–road noise, with the corresponding source heights.

The ground effect for the inversion process is estimated in the same manner as the air attenuation, except that also the source height is considered. Using the above described transition frequency, the different frequency bands are identified with the corresponding source height. Modelling the recording situation with a receiver height of 1.5 m, a pass-by distance of 7.5 m, and a dense asphalt ground, the ground effect is estimated.

Resulting from the inversion process is a signal that is seen as a steady-state source signal shaped by a source directivity. The slowly varying amplitudes (envelopes) of each third-octave band are stored as directivity polynomials for later use in the auralization. After separation into forward and backward direction, a second-degree polynomial fitting is used with an adjustment to also fit the centre level in order to give a continuous curve. After removing the variation in amplitude modelled as directivity, a period shortly after point of passage is used as an estimate of the source signal. As default, a 1 s long signal was used, starting 1 s after point of passage. The reason for here avoiding the point of passage is that, even though the modelled directivity is removed, amplitude variations still exist and are usually largest near point of passage. The purpose of using the signal after point of passage, rather than before point of passage, is to ease the capture of the propulsion sound's tonal character, which is usually more prominent toward the rear of the vehicle where the exhaust is located.

In a first approach, the propulsion sound signals were decomposed into a set of tones and a noise part, where the amount of tones were limited to one per third-octave band.

The first round of listening tests within the LISTEN project investigated, among other things, the importance of including the tonal part, with the conclusion that including the tonal components gave an overall better result than omitting them, in terms of perceived speed, annoyance and realism, however at a small and non-systematic effect [3]. An update in the modelling of the tonal character was made, based on so-called granular synthesis [20], with the idea to find the shortest time pattern that describes the propulsion sound. Within the project, this was made using auto correlation analysis, resulting in an average time pattern. The amplitude of the grain was adjusted to give the same tonal power as in the first approach, and the noise part was kept the same. A second set of listening tests showed that the auralization method had been improved [4], and this final approach is here referred to as the LISTEN model. For application to other road surfaces or tyres, the third-octave spectrum used here for the tyre–road noise can be exchanged.

2.4 Summary of previous validation of the auralization approach

The above described method for auralizing road traffic, implemented in Matlab, was subjected to validation by listening tests within the LISTEN project [4,5], for which the main results are summarised here.

A discrimination listening test was made using the five pass-by recordings, resulting in an average proportion of correct responses below 0.75 for the 2 s long middle parts of the sounds, whereas the 2 s long excerpts for, respectively, approaching and leaving vehicles gave a higher proportion of correct responses [4]. In a detection test, using 6 s long passages, the average proportion of correct responses was 0.75–0.83 for the different driving speeds, using feedback on whether the sound played was recorded or synthesised [4]. A proportion of correct responses around 0.75 is interpreted as a rather good result. It is in between the ideal result (0.5), which would correspond to guessing at random, and the worst result (1.0), which would correspond to always knowing if the sound was recorded or synthesised; hence a listener guessing at random half of the time and knowing half of the time would give a 0.75 proportion of correct responses.

Another set of listening tests was made on comparing annoyance and perceived speed between recordings and their respective auralization, resulting within a 0.25 variability from the ideal result (0.5) for the five pass-by sounds [4].

To conclude the previous study, it was stated to provide support for the validity of the LISTEN approach to auralization [4].

3. Modelling tyre–road sound

The main idea of the modelling approach used here is the combination of a physical model of the contact forces between tyre and road and a statistical model describing the connection between contact forces and sound pressure levels for the controlled pass-by (CPB) situation.

3.1 The statistical model

The starting point is the assumption that the measured pass-by values stem from three different sources:

- Tyre vibrations due to the excitation of the tyre structure (p_{vibr}^2)
- Air-flow related mechanisms due to aerodynamic processes in the contact zone (p_{air}^2)

- Flow noise due to the flow around the vehicle body ($p^2_{residual}$)

The sound pressure level in each third-octave band is then given as a combination of the following three contributions

$$Lp = 10 \log_{10} \left(\frac{p^2_{vibr} + p^2_{air} + p^2_{residual}}{p^2_{ref}} \right) \quad \text{Eq 6}$$

where $p_{ref} = 2 \cdot 10^{-5}$ Pa. For each of the terms, an assumption about the influence function is made containing a series of variables. For tyre vibrations the contribution is assumed to follow

$$p^2_{vibr} = a_1 F_c^k \quad \text{Eq 7}$$

where a_1 is an unknown factor for each third-octave band and k is an unknown exponent while F_c are pre-calculated contact forces, dependant on rolling speed, delivered by the physical model.

The term belonging to air-flow related mechanisms is

$$p^2_{air} = a_2 F_c^m s^{-m} R_s^n U^o \quad \text{Eq 8}$$

where a_2 is and unknown factor for each third-octave band, m, n and o are unknown, real-valued exponents, s is the tread stiffness measured for each tyre as shore hardness, R_s is the flow resistance of the road surface and U is the rolling speed. For further information on the input parameters see [6]. Finally, the residual term is written as

$$p^2_{residual} = a_3 U^p \quad \text{Eq 9}$$

where the factor a_3 is determined for each third-octave band from wind tunnel measurements for the vehicle used in the measurement campaign. The unknown exponents k, m, n, o and p as well as the unknown factors a_1 und a_2 are determined from Eq. (6). For this, more than 1000 field measurements under very controlled conditions are used. These measurements were carried out on special test surfaces on a former airfield close to Berlin [21]. As a complete documentation of these measurements exists, it is possible to use the tyre–road model developed at Chalmers (see following Section) to calculate the contact forces for these 1000 cases. The calculated contact forces are then used to find the best fit of Eqs. (6–9) between calculated forces and measured pass-by levels for each third-octave band.

3.2 The prediction model for contact forces

The prediction model consists of two parts, the tyre model (Section 3.2.1) and the contact model (Section 3.2.2).

3.2.1 Tyre model

A simplified tyre model has been used for the establishment of the model [22]. Since more than 1000 cases had to be calculated, it had to be simple and efficient. Furthermore, the variety of tyres required to update the model based on measurements. This is only possible if the number of parameters is kept low. The tyre system is therefore modelled as an orthotropic plate on elastic support [6]. It has both the advantages of being handy and of being sufficiently accurate in the frequency range up to 4 kHz. The main idea is that the belt and the two sidewalls of the tyre form a flat plate with different bending stiffness in longitudinal and lateral direction (see Figure 1).

The differential equation for the vertical motion of the plate is:

$$T_0\left(\frac{\partial^2\xi}{\partial x^2}+\frac{\partial^2\xi}{\partial y^2}\right)+B_x\frac{\partial^4\xi}{\partial x^4}+B_{xy}\frac{\partial^4\xi}{\partial x^2\partial y^2}+B_y\frac{\partial^4\xi}{\partial y^4}+m''\frac{\partial^2\xi}{\partial t^2}+K\xi=F_0''. \qquad \text{Eq 10}$$

The plate is under the tension T_o, caused by the interior air pressure of the tyre, has the bending stiffness B_x in circumferential direction and the bending stiffness B_y in lateral direction. B_{xy} is the cross stiffness and can be well approximated by $B_{xy} \approx \sqrt{B_x B_y}$. Here, ξ is the vertical displacement of the plate, i.e. the radial displacement in the tyre coordinates. The elastic foundation of the belt is represented by the spring stiffness K, m'' is the mass per cross section and F_o'' is the acting force per cross section. A modal approach is used to solve the equation, with basis functions in the form of $\cos(2n\pi x/L_x)\sin(m\pi y/L_y)$ where L_x is the tyre width (from beat to beat) and L_y is the circumference. The variables *n* and *m* are the number of half wave lengths fitting to L_x and L_y.

Comparison of the model with measurements shows a surprisingly good agreement as long as:

- The excitation area is not to small – otherwise the local stiffness, which is not included in the model, needs to be considered
- One has an accurate set of material properties for establishing the parameters of the plate system in this model.

The model has also the following limitations (with possible remedies in parenthesis):

- The shift of the resonance frequencies for the range below the ring frequency. The shift is caused by the neglecting the circumferential curvature of the real-life structure. (However, the shift can be compensated by frequency dependent material parameters.)
- Similar problems occur due to neglecting the lateral curvature (but can be cured in the same way)
- In addition, the model can only be used for a frequency range up to about 4000 Hz. At this frequency the thickness, *h*, of the plate is comparable with the wavelength λ_B of the bending waves.

Despite these restrictions, the model of the orthotropic plate is a simple and useful tool to describe the structure-borne sound properties of a tyre with a low numerical effort.

A big advantage of the model is the limited number of input data required for the model. These data are:

- The mass per unit area of the tyre structure
- Radial bedding stiffness dependent on the inflation pressure and the sidewall stiffness
- Tension dependent on the inflation pressure
- Circumferential bending stiffness
- Lateral bending stiffness
- Additionally, damping has to be determined as a complex modulus for the different stiffness terms.

Table 1 shows an example of values for the material data used in Eq. (10). For this a comparison of measurement and calculations is made.

Based on such data, a very good performance of the model can be achieved. Figure 2 shows the comparison of measured and calculated frequency response functions for a typical commercial tyre.

3.2.2 Contact Models

At a larger scale, the interaction of elastic bodies can be studied by applying models like contact stiffness or friction coefficients having their origin in the physics behind the interaction of molecules. It is this scale for which today's contact models are mainly formulated.

As a first starting point one could think about the tyre as a structure where a Winkler bedding is added (i.e. a model of isolated springs). These springs represent the local contact stiffness due to the interaction between the road surface and the rubber tread of the tyre. The contact forces at any point in the contact zone are consequently given by the stiffness of the bedding and its compression. The compression of the spring $\Delta y_e(\varphi_e,t)$, at the angle φ_e is a function of the centre of the rim $y_0(t)$, the curvature $k_2(\varphi_e)$ of the tyre, the vibration $\xi_e(\varphi_e,t)$ of the tyre belt and the roughness $k_{10}(\varphi_e,t)$ of the road:

$$\Delta y_e(\varphi_e,t) = y_0(t) + k_{10}(\varphi_e,t) + \xi_e(\varphi_e,t) - k_2(\varphi_e) \quad \text{Eq 11}$$

Eq. 11 describes the geometry between tyre and road. If the tyre would penetrate the road surface, the distance $\Delta y_e(\varphi_e,t)$ would be negative. Only in this case a force is acting on that part of the tyre. The contact force is then

$$F_e(\varphi_e,t) = s\Delta y_e(\varphi_e,t)H\left[-\Delta y_e(\varphi_e,t)\right] \quad \text{Eq 12}$$

where H is the step function switching contact on and off depending on $\Delta y_e(\varphi_e,t)$ and s, the contact stiffness. Since the motion of the tyre is a function of the forces, a non-linear equation system has to be solved for each time step in order to obtain the contact forces,

$$\xi_e(\varphi_e,t) = \sum_{m=1}^{M} F_m(\varphi_m,t) * g_{m,e}(t) \quad \text{Eq 13}$$

where $g_{m,e}(t)$ is the impulse response function of the tyre structure at position e due to an impulse at position m. It represents the convolution between all contact forces and the corresponding impulse response functions. The implementation in the time domain allows for considering non-linear stiffness for the contact or relaxation of the rubber material.

A more detailed description of this can be found in e.g. [23]. In such a model only contact forces normal to the surface are considered. To speed up calculation times, an extension to three dimensions has been made by Wullens [24]. Eq. (12) can be formulated in a general way, for the cases where the tread is not modelled as isolated springs as

$$\mathbf{F} = \mathbf{G}^{-1}\Delta\mathbf{y} \quad \text{Eq 14}$$

In this case $\mathbf{G}$ is the sensitivity matrix describing how strong the reaction at different positions is due to a force applied at a certain position. Since the matrix has to be inverted only those points which actually are in contact need to be considered. Unfortunately this is not known from the beginning and therefore an iterative process has to be carried out to find the correct solution of the force distribution. This iteration process will deliver the correct contact geometry and the correct contact forces for each time step. There are different possibilities to model $\mathbf{G}$, e.g. from the deformation of an elastic half space or the deformation of an elastic layer of finite thickness.

Although Wullens showed in [23] that the full three dimensional model works fine, it is not suitable for the purpose here due to its computational effort of several hours for one case (i.e. a limited number of tyre revolutions under given load and speed). The reduction to a two-dimensional roughness might be attractive having in mind also that the description of the road surface texture would be much easier (e.g. only measurements along one track would be needed). However, the lateral roughness distribution is important to properly estimate the interaction forces (see [25]). Therefore the so-called "quasi three dimensional contact model" has been developed for the approach here.

The main idea is that when a piece of rubber is pressed on a rough surface, the resulting local contact force will be proportional to the rubber area in contact with the rough surface as shown in Figure 3. From this the nonlinear stiffness function, s_e, is calculated.

This leads to a non-linear stiffness depending on the lateral roughness distribution of the road surface. The resulting local contact force $F(t,\varphi_e)$ is now

$$F(t,\varphi_e) = \int_o^{\Delta y_e(\varphi_e)} s_e(\eta)\,d\eta \qquad \text{Eq. 15}$$

where Δy_e is the indention depth. In this way the lateral roughness pattern of the road is translated into a variation of the characteristic function of the non-linear bedding stiffness. For each slice of the tread, such a characteristic function is calculated. In this way, the circumferential variation of the roughness including the lateral characteristics of this change is taken into account. This complication of the previous model does however not cause largely increased computational cost since the values of the integral can be pre-calculated and interpolation routines can be used to read values in between pre-calculated ones.

Figure 4 (left) shows a typical roughness distribution over the width of the tread and as function of the 'slice' number (in this case the circumference is divided in 512 slices corresponding to 3.4 mm width of each slice). On the right hand side of the figure the corresponding stiffness functions are displayed.

The stiffness K_0 represents the tread stiffness of the tyre. This quantity is measured for each individual tyre involved in the model and modified according to the spatial resolution. Typical values of the stiffness are in the order $2\ 10^4$ N/m.

The roughness is measured in six parallel tracks, which has been shown to be a sufficient statistical description of the road texture as long as the texture is not an

artificially created texture with strong anisotropy. However, in this case the number of measured tracks can be increased to ensure a good description of the lateral roughness distribution.

From the simulations, the contact force distribution can be obtained. In Figure 5 the simulated total normal contact force as function of time is shown, i.e. the sum over all local contact forces. The total contact force is then used for the evaluation of the statistical model. As roughness was only measured over a length of two meters, a longer record was created by adding several of these pieces in sequence. In order to avoid discontinuities at the interface between two pieces, every other record was horizontally flipped, i.e. effectively time reversed. The first part is the loading process. Then the tyre starts to roll. After a few revolutions the tyre reaches a "steady state condition" and the contact force is only a function of the roughness variation in the contact. The results are shown for a surface from the Sperenberg project and for a rolling speed of 70 km/h. The last part of the total contact force (150 ms) is then used to calculate the contact spectra.

The calculated contact force spectra in third-octave bands are input into the statistical model. For determining the unknown parameters from Section 2, more than 1000 cases were calculated. From these the model equations (6–9) were extracted. These models can be used to predict third-octave band levels as function of tyre, road surface roughness, rolling speed and load.

An example showing the quality of such prediction is given in the following Section. However, due to the set-up of the model there is a natural limitation with regards to the applicable frequency range. At low frequencies the frequency resolution is too low for achieving reliable results in third-octave bands. The high frequency limit is given by the maximum frequency considered in the contact model, which is formulated in the time domain.

The simulation model has been applied in a series of projects and besides others compared with the so-called HyRoNE model (see e.g. [6]). The uncertainty of the model is in the order of ± 1 dB in overall level, but can vary in special cases up to a few dB in the lower third-octave bands.

4. The combined auralization tool

The combined auralization tool uses the models of LISTEN and SPERoN presented in previous sections 2 and 3, respectively. For this, the LISTEN source data related to the tyre–road noise, given in third-octave bands, is modified by using SPERoN results. SPERoN delivers the estimated sound pressure levels for the third-octave bands 315–2000 Hz. These levels are adjusted to match the ones of the LISTEN source data. This means that the sound power level is estimated and a fixed offset is applied. This initial auralization approach works fine when using the original LISTEN values for all bands where no data is available from SPERoN, as shown below.

However, to consider wind noise and to reach an even better match with recordings under similar conditions, further adjustments were included in the combined auralization. Spectral comparisons were made between recorded pass-by sounds and those generated using the initial auralization approach, showing discrepancies with the largest deviations appearing in the low-frequency bands, which leads to the conclusion that wind noise is underestimated. Improvement values for the third-octave bands were

chosen in a way that the resulting auralization matches with corresponding real recording of pass-by at 7.5 m distance in terms of the spectrum at the maximum level (L_{AFmax}). This was made considering a set of recordings and auralizations and then applied equally to all following cases. The improvement was made slightly differently for different frequency regions: bands below 315 Hz, bands above 2000 Hz, and the remaining bands, i.e. where SPERoN delivers values.

For the frequency bands below 315 Hz the levels are based on the 315 Hz-value from SPERoN. For frequencies of 250 Hz down to 125 Hz, values are decreasing. For lower frequencies, the levels are stepwise increased again. The resulting adjustments, for a driving speed of 50 km/h, are: 0.9 dB at 250 Hz; 0.6 dB at 200 Hz; 0.3 dB at 160 Hz; and from 125 Hz down to 31.5 Hz the values are changed in steps of 0.5 dB from -1 dB to 2 dB. The value for the lowest band (20 Hz) was 12 dB. For lower speeds the above values are decreased and for higher speeds they are increased, to match the measured increase in wind noise with speed.

For the frequency bands above 2000 Hz, the levels from the LISTEN source data were used, but with a corresponding offset adjustment to match the SPERoN levels. This is shown in Figure 6 for one tyre–road combination to illustrate the adjustment. Shown are the third-octave band values stored in the LISTEN source data for the tyre–road noise ('reference data'), the source data after including the values given by SPERoN ('old data') and the final auralization model ('new data').

With this approach, the LISTEN tyre–road noise source-term can be shaped by the spectra estimated in SPERoN and synthesized back into a pass-by signal. Figure 7 shows the auralization process. The initial approach lacks the stage that is highlighted with the box.

5. Implementation and testing

5.1 General setting

For binaural listening, the signal is processed with head related transfer functions (HRTF). Open source KEMAR dummy head recordings were used [26], taking into consideration the effect of the ear canal. These recordings provide HRTFs with an angular resolution of 5 degrees in the horizontal plane. To apply appropriate HRTF, for each sample of the sound source, the angle between the listener and the sound source is calculated. These values are then rounded to the given five-degree steps. Thus, for each sample the appropriate HRTF is chosen. No audible artefacts were detected.

Each of the utilized models has been validated during its development. The combined auralization tool is validated on the basis of how well the perception of the generated sounds matches the perception of corresponding recordings. The listening tests were designed as a seven-step semantic differential. The participants were asked to rate a set of different perceptual attributes, of which we here focus on pleasantness. For each tested signal and each attribute, the participants were asked to rate on a scale from 1 to 7 as to how much they agree that the attribute describes the sound.

The simulations were using tyre–road noise only, without engine and other propulsion sounds. The used recordings were coast-by measurements, i.e. with engine turned off. Both simulations and recordings were at a distance of 7.5 m at the moment of pass by and at a speed of 50 km/h. In all tests, the same nine tyre–road combinations have been

used. The participants were all non-experts, but most of them had already participated in a number of listening tests.

5.2 Pre-study

In a pre-study, using the initial auralization approach, nine simulated and recorded signals were evaluated in two separate listening tests. In the first listening test, the simulated signals were presented via two loudspeakers in a sound-insulated room furnished as a lecture room. The participants were listening in groups of maximum three participants at a time and receiving the questions on paper. In total, 14 participants (7 male, 7 female) participated in the listening test (age: mean=28 years, s.d.=5.1 years). The second listening test was set up on a computer and the recorded sounds were presented via open headphones (Sennheiser HD 650, calibrated using a HEAD acoustics dummy head) in a soundproof and neutral room. In total 18 participants (9 male, 9 female) participated in this second listening test (age: mean = 26 years, s.d. = 3.3 years). In both listening tests the signals were randomized.

The pre-study indicated a fair match between auralized and recorded sounds in perception of pleasantness (Figure 8). The correlation coefficient is R=0.73. This leads to a probability of P=0.026 that the null-hypothesis of no correlation between the signals is true.

5.3 Main study

The main validation study focused on the final auralization model. Recorded and auralized signals were used for a speed of 50 km/h. The recorded signals were calibrated on their maximum sound pressure level (L_{AFmax}). The listening test was performed in a neutral, sound-insulated and damped room and the sounds were presented via Sennheiser HD 650 headphones (calibrated via a HEAD acoustics dummy head). The playback of the signals was randomised. In total, 18 participants (9 male, 9 female) participated in the listening test (mean age = 26 years, s.d. = 3.3 years).

Figure 9 contains the results. They show that the final model, adjusted with consideration of the wind noise, gives a better agreement in pleasantness between recordings and simulations than the pre-study. This type of agreement, i.e. within one experiment, is of main importance, whereas it could be noted that between the two experiments the average level of pleasantness for the auralized sounds is different, which may be due to the differences of the playback situations. For the final model the correlation was increased to R=0.77 and P=0.015. To conclude, the agreement shows a successful validation of the auralization methodology.

6. Conclusion

The purpose of this paper is to introduce a tool for tyre–road noise auralization of cars in a pass-by situation. To include proper descriptions of the sources and to model the propagation path from the moving vehicle to a listener, two models are combined. The first model approach concerns the auralization of pass-by sound from road vehicles and has been developed in the Swedish national LISTEN project. In this model the source signals for engine and tyre–road interaction, constructed from recorded data, are separated from the propagation effects. This gives the possibility to modify both the source signals and the sound propagation to a listener.

The second model approach concerns the prediction of third-octave band levels of rolling noise for different tyre–road combinations. This model is built on work made

inside the Sperenberg project and is known as the SPERoN model. The combination of both models allows simulation and auralization of pass-by sounds for arbitrary tyre–road combinations, as long as dense road surfaces are considered.

First listening tests show promising results. The generated signals were compared to recordings, for an initial and a further refined approach to combine the two models. For the final model, the resulting sounds are perceived similar to recordings in pleasantness. Thereby a potentially powerful tool for the auralization of tyre–road noise is provided, however further listening tests are needed for a thorough validation of the proposed method. Concerning future work, the final model, as presented here, can be further developed to include heavy-duty road vehicles as well as to model accelerating vehicles.

Acknowledgement

We are grateful the co-workers of the LISTEN project, coordinated by Mats Nilsson (at Department of Psychology, Stockholm University, Sweden). We would also like to thank Tomasz Kaczmarek (at Adam Mickiewicz University, Poznań, Poland) for providing the pass-by recordings. Furthermore, we would like to thank the German Federal Highway Research Institute (BAST) for the support of this research within the Project *Silent road traffic noise 3 (Leiser Straßenverkehr 3)*.

References

[1] Keulen, W. van and Duskov, M. Inventory study of basic knowledge on tyre / road noise. Report, Poject report DWW-2005-022, IPG, 2005.

[2] Burden of disease from environmental noise. Quantification of healthy life years lost in Europe. WHO, 2011.

[3] Forssén, J., Kaczmarek, T., Alvarsson, J., Lundén, P. & Nilsson, M. (2009) Auralization of traffic noise within the LISTEN project – Preliminary results for passenger car pass-by. Euronoise 2009.

[4] Nilsson, M., Rådsten-Ekman, M., Alvarsson, J., Lundén, P. & Forssén, J. (2011) Perceptual validation of auralized road traffic noise. Inter-Noise, Osaka, Japan, 40th International Congress and Exposition on Noise Control Engineering, September 2011.

[5] Nilsson, M., Forssén, J., Lundén, P., Peplow, A. & Hellström, B. (2011) *LISTEN – Auralization of Urban Soundscapes. Final report to the Knowledge Foundation*.

[6] T. Beckenbauer, P. Klein, J. Hamet och W. Kropp, "Tyre/road noise prediction: A comparison between the SPERoN and HyRoNE models, part 1" (Acoustics 08, Paris, June 29-July 4, 2008), 2008.

[7] Maillard, J., Martin, J. A simulation and restitution technique for the perceptive evaluation of road traffic noise. Proc. Euronoise, Paris, 2008.

[8] Kaczmarek, T., Road-vehicle simulation for psychoacoustic studies, in International Congress of Acoustics. 2007, International Commission for Acoustics: Madrid.

[9] Jagla, J., Maillard, J., Martin, N. Sample-based engine noise synthesis using an enhanced pitch-synchronous overlap-and-add method, Journal of the Acoustical Society of America, 132(5), pp. 3098-3108, 2012

[10] Pieren R, Bütler T, Heutschi K. Auralization of Accelerating Passenger Cars Using Spectral Modeling Synthesis. Applied Sciences. 2016; 6(1):5.

[11] Bergman, P., Pieringer, A., Forssén, J., Höstmad, P. Perceptual validation of auralized heavy-duty vehicle. Proc. Euronoise 2015, Maastricht, June 1-3, 2015

[12] Arntzen, M., Simons, D. G. Ground Reflection with Turbulence Induced Coherence Loss in Flyover Auralization. International Journal of Aeroacoustics (13), 2014.

[13] Plovsing, B., Proposal for Nordtest Method: Nord2000 – Prediction of Outdoor Sound Propagation. Nordtest Proposal AV 1106/07. 2007, Hørsholm, Denmark: Delta.

[14] Nota, R., R. Barelds, and D. van Maercke, Engineering method for road traffic and railway noise after validation and fine-tuning (Technical Report HAR32TR-040922-DGMR20). 2005: EC under the Information Society and Technology (IST) Programme.

[15] ISO 9613-1: Acoustics—Attenuation of Sound During Propagation Outdoors—Part 1: Calculation of the Absorption of Sound by the Atmosphere. ISO, 1993.

[16] van Maercke, D. and Defrance, J., "Development of an analytical model for outdoor sound propagation within the Harmonoise project," Acta Acustica united with Acustica **93** (2), 201-212 (2007).
[17] Clifford, S.F. and Lataitis, R.J. Turbulence effects on acoustic wave propagation over a smooth surface. J. Acoust. Soc. Am., Vol. 73, 1983, pp. 1545-1550.
[18] Ostashev, V.E., et al., Propagation of sound in a turbulent medium. II. Spherical waves. . Journal of the Acoustical Society of America, 1997. 102: p. 2571-2578.
[19] Jonasson, H., "Acoustical source modelling of road vehicles," Acta Acustica united with Acustica 93 (2), 173-184 (2007).
[20] Roads, C., Introduction to granular synthesis. Computer Music Journal, 12(2), 1990.
[21] Forschungsbericht FE-Nr. 03.293/1995/MRB „Einfluss der Fahrbahntextur auf das Reifen-Fahrbahn-Geräusch", 2001
[22] W Kropp, Structure-borne Sound on a Smooth Tyre, Applied Acoustics **26** (1989), 181-192.
[23] Wullens, F; Kropp, W. A three-dimensional contact model for tyre/road interaction in rolling conditions, Acta Acustica United with Acustica. 90 (4). p. 702-711, 2004, Number of citations: 68
[24] Wullens, F., Kropp, W., Jean, P. Quasi-3D versus 3D contact modelling for tyre/road interaction. Inter-Noise Prague. 22-25 August, 2004
[25] Hoever, C., Kropp, W. The influence of lateral road surface resolution on the simulation of car tyre rolling losses and rolling noise, Proceedings of Inter-Noise 2013,
[26] B. Gardner and K. Martin. HRTF Measurements of a KEMAR Dummy-Head Microphone. MIT Media Lab, Machine Listening Group, 1994.

Table

Tyre width	L_y	0.355m
Tyre circumference	L_x	1.97m
Mass per m^2	m''	12 kg/m^2
Radial bedding stiffness	K	3.6 10^6 N/m^3
Tension	T_0	74160 N/m
Bending stiffness in x-direction	B_x	9 Nm
Bending stiffness in y-direction	B_y	7.2 Nm
Mixed bending stiffness	B_{xy}	8 Nm

Table 1. Example of material data for the tyre model in Eq. (10).

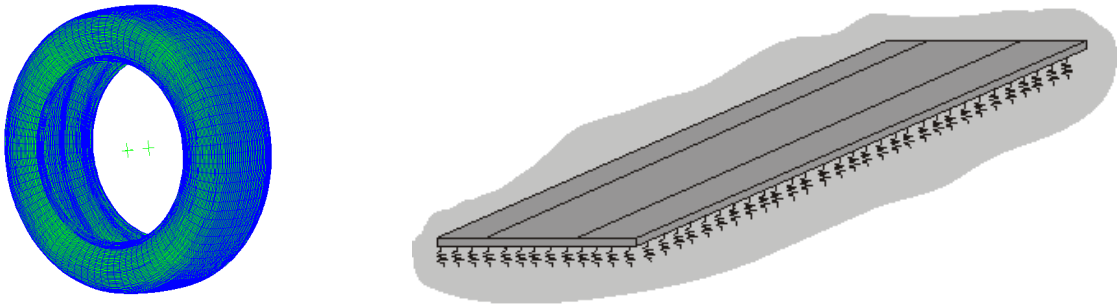

Figure 1. Simplified geometry of the orthotropic plate model. Sidewalls and tread build one flat plate. The support by inflation pressure and sidewalls are simulate by an elastic bedding.

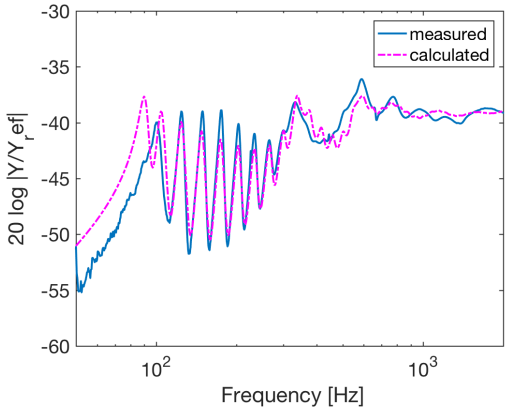

Figure 2. Comparison between calculated and measured radial frequency response to a unit force acting in the middle of the tread. Y_{ref}=1 m/sN.

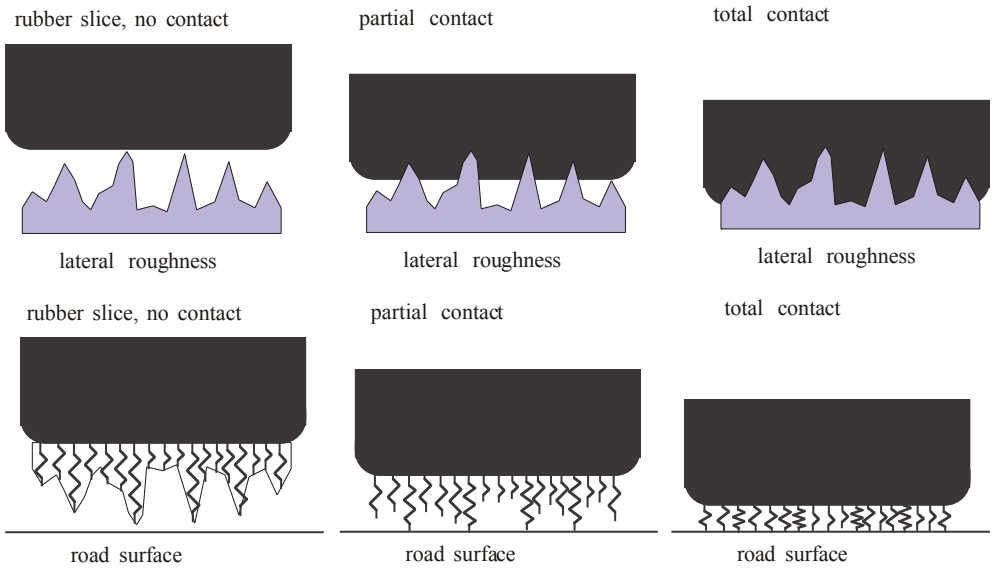

Figure 3. Schematic presentation of a lateral rubber slice in no, partial, and total contact with the road surface (upper Figure) and modelling as a Winkler bedding system (lower Figure).

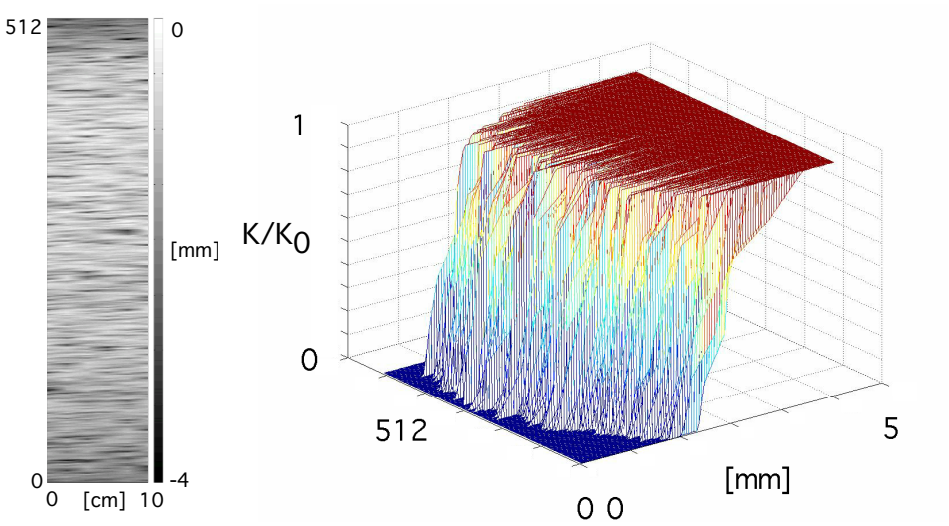

Figure 4. Example of a 3D roughness pattern (left) and the corresponding stiffness (right) of the bedding (normalised by the stiffness for total contact over the width of the tyre).

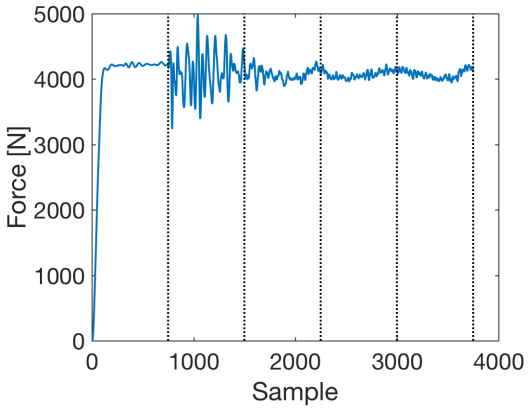

Figure 5. Total normal contact force as function of time samples for a surface from the Sperenberg project at a speed of 70 km/h (time between samples is 0.14 ms). The last part of the total contact force (150 ms) is then used in the evaluation.

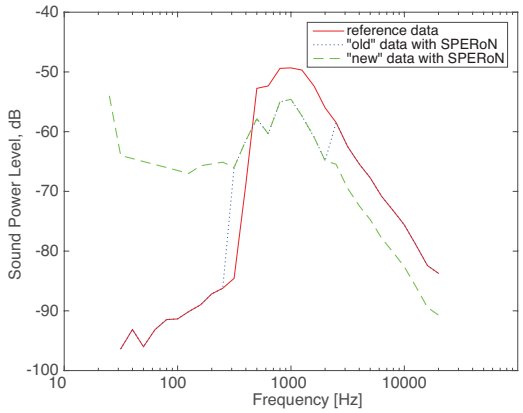

Figure 6. Third-octave band values of the LISTEN source data ('reference data'), third-octave band values after replacing the values from 315 Hz to 2000 Hz by the values given by SPERoN ('old data with SPERoN') and third-octave band values for the final combined auralization model ('new data with SPERoN') for one tyre road combination (A1).

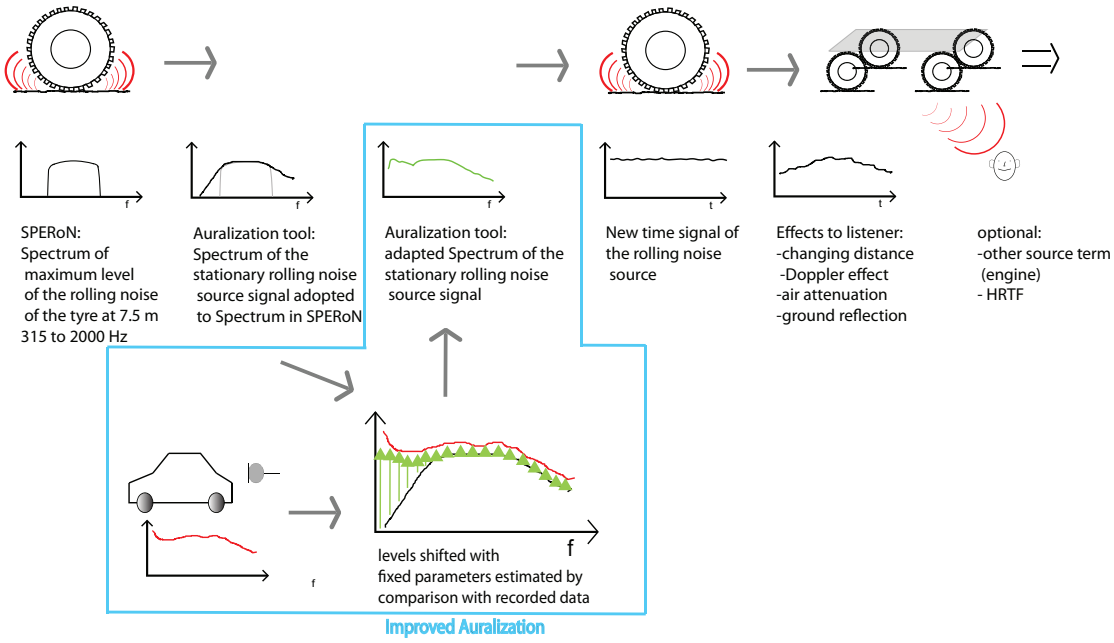

Figure 7. Illustration of the auralization process: SPERoN estimates the rolling noise spectrum out of basic properties of tyre and road; the source terms in the auralization are compared with the calibrated spectrum and fitted to the new source; calibration factors estimated from comparison with recordings are applied for each frequency band; propagation effects are added to the source term and a pass-by signal is generated for such desired conditions as distance, speed, and surrounding.

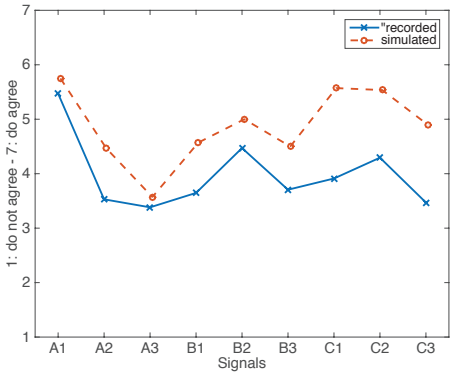

Figure 8. Comparison between the responses in the listening tests between recorded and auralized signals for the perceived pleasantness for the initial auralization model.

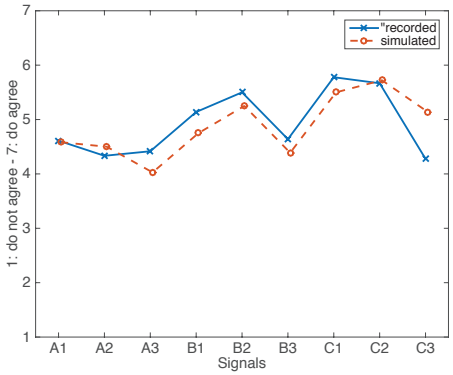

Figure 9. Comparison between the responses in the listening tests between recorded and auralized signals for the perceived pleasantness for the final auralization model.